DOI: 10.3901/CJME.2014.0616.109, available online at www.springerlink.com; www.cjmenet.com; www.cjmenet.com.cn

Physics-based Modeling and Simulation for Motional Cable Harness Design

LIU Jianhua*, ZHAO Tao, NING Ruxin, and LIU Jiashun

School of Mechanical Engineering, Beijing Institute of Technology, Beijing 100081, China

Received October 17, 2013; revised June 9, 2014; accepted June 16, 2014

Abstract: The design work of motional cable in products is vital due to the difficulty in estimating the potential issues in current researches. In this paper, a physics-based modeling and simulation method for the motional cable harness design is presented. The model, based on continuum mechanics, is established by analyzing the force of microelement in equilibrium. During the analysis procedure, three coordinate systems: inertial, Frenet and main-axis coordinate systems are used. By variable substitution and dimensionless processing, the equation set is discretized by differential quadrature method and subsequently becomes an overdetermined nonlinear equation set with boundary conditions solved by Levenberg-Marquardt method. With the profile of motional cable harness obtained from the integral of arithmetic solution, a motion simulation system based on "path" and "profile" as well as the experimental equipments is built. Using the same parameters as input for the simulation and the real cable harness correspondingly, the issue in designing, such as collision, can be easily found by the simulation system. This research obtains a better result which has no potential collisions by redesign, and the proposed method can be used as an accurate and efficient way in motional cable harness design work.

Keywords: motional cable harness, physics-based modeling, motion simulation, Kirchhoff rod

1 Introduction

Cable harnesses are widely used in electro-mechanical products with the development of electronic and optical communication technology. The function of cable harness is to transport signal and power. The product will not be able to work if the cable harness is malfunctioning. Therefore, the design rationality of cable harness is very important to the quality of products.

There is a special type of cable harness named motional cable harness, which is able to move while the connected part is moving. Several problems, including bending scathe, fatigue scathe and collision with other parts, are related to motional cable harness because of the weakness in design method. Motional cable harness design is usually at the end of the whole product design circle and is carried out by repeatedly testing of the physical prototype, which increases the cost as well as designing time and reduces the reliability at the same time. Thus establishing a physics-based model and simulating the motion process of motional cable harness in virtual environment become an effective method for the problems mentioned above.

Some related work using different approaches is listed below. RABAETJE[1] reported a kind of spring-mass model and LEON, et al[2], used a kind of finite element model to simulate the deformation of the cable. LOOCK, et al[3], proposed a kind of mass-spring model with generalized springs to obtain a physically plausible real-time simulation for cables with moderate complexity. HERGENROTHER, et al[4], presented an algorithm by inverse kinematics. The cable is modeled by consecutive cylinder segments and ball joints connecting the segments. QI, et al[5], presented a physical beam-bending model to simulate the behavior of the elastic tube. SANG, et al[6], proposed a method based on the shape-retaining chain linked model that can handle the deformation of flexible object. SEONGKI, et al[7], proposed a continuum mechanics-based finite element adaptive method to perform a haptic interaction with a deformable object. Most models presented are not accurate enough because they cannot describe the twisting of motional cable harness accurately.

The kinetic analogy was proposed in 1859 by Kirchhoff. It is the base of statics of an elastic rod. The elastic rod model can be used as the mechanical model for many objects, such as rope, drill pipe, fiber, caudex of climbing plants, and so on. In the oceanographic cable field, ZAJAC[8], COHEN[9], JAMES[10], KNAP[11–12], COYNE[13], LE[14], MIYAZAKI, et al[15], studied the equilibrium stability of rod with round cross section. VAN, et al[16–18], studied the flexuosity of rod with no round cross section. For drill pipe, SEEMANN[19], VAN, et al[20–22], studied the equilibrium and stability of elastic rod constrained to a plane and cylinder. In the molecular biology field, BENHAM[23–24] and LE[25–26] established a model of DNA based on Kirchhoff's elastic rod theory. Though, to our best

* Corresponding author. E-mail: jeffliu@bit.edu.cn
Supported by National Natural Science Foundation of China (Grant No. 51275047)

knowledge, no application of elastic rod theory in motional cable harness simulation has been proposed yet.

This paper consists of seven parts. The first part is the introduction and the second is the description of the modeling process. The equation set solved by the numerical solution method is described in the third part. Then a motion simulation method based on the proposed model is introduced in the fourth part. In the fifth part, a set of experimental equipment is described for the validation. The new prototype system developed is introduced in the sixth part and the conclusion is the last part.

2 Physics-based Modeling Method

The motional cable harness is considered to be a one-dimensional body instead of a three-dimensional body. It can be described by its centerline. The basic assumptions are as follows: (1) The motional cable harness is homogeneous, inextensible, unshearable, isotropic and linearly elastic. This can simplify the analysis without any impact on the continuity of the cable. Actually, these limitations can be released as the research continues. (2) The cross section is uniformly rounded, rigid and perpendicular to the centerline. That means only round section cable harness is discussed in this paper. (3) The length and curvature radius are far larger than the radius of cross section. This is the most situation of the motional cable harness.

LIU[27] studied the rod with discretionary cross section. The physical character oriented model described in this section can be obtained on the analogy of Liu's study. The reference frames and the force on microelement of motional cable harness are shown in Fig. 1.

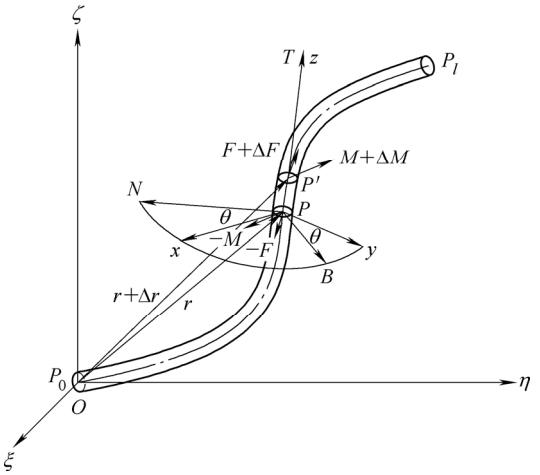

Fig. 1. Reference frames and the force on microelement of motional cable harness

Where in Fig. 1,

$O\xi\eta\zeta$—Descartes inertial coordinate system. Point O is the origin. The direction of axis ζ is vertical,

$PNBT$—The Frenet coordinate system. N is normal, B is binormal and T is tangent,

$Pxyz$—The main axis coordinate system. Axis z superpose axis T,

θ—Angle between axis x and axis N, and between axis y and axis B. It means that the main axis coordinate system can be obtained by rotating the Frenet coordinate system along axis z by θ degrees,

P_0—The fixed point of motional cable harness,

P_l—Moving point of motional cable harness,

P—Discretionary point on the centre line of motional cable harness,

P'—Point closes to P unlimitedly,

$\boldsymbol{R}$—Radius vectors from O to P,

$\boldsymbol{r}+\Delta\boldsymbol{r}$—Radius vectors from O to P',

$-\boldsymbol{F}$—The main vector of inner force on microelement PP' at point P,

$-\boldsymbol{M}$—The main vector of inner moment on microelement PP' at point P,

$\boldsymbol{F}+\Delta\boldsymbol{F}$—The main vector of inner force on microelement PP' at point P',

$\boldsymbol{M}+\Delta\boldsymbol{M}$—the main vector of inner moment on microelement PP' at point P'.

An arc-coordinate system is established along the motional cable harness. The origin of the arc-coordinate is P_0. When the force on microelement are in equilibrium, the inner force and moments predigesting to P is zero. Divided by Δs, when $\Delta s\to 0$ the equilibrium functions can be described as

$$\frac{\mathrm{d}\boldsymbol{F}}{\mathrm{d}s}=\boldsymbol{0}, \tag{1}$$

$$\frac{\mathrm{d}\boldsymbol{M}}{\mathrm{d}s}+\boldsymbol{T}\times\boldsymbol{F}=\boldsymbol{0}, \tag{2}$$

where s—Arc-coordinate of P,

$\boldsymbol{T}$—Base vector of tangent at P.

Make the differential coefficient process in main axis coordinate system. Bring the projection of $\boldsymbol{\omega}$ (curvature-twisting vector), $\boldsymbol{F}$ and $\boldsymbol{M}$ into equations. Eqs. (1) and (2) can be written as

$$\boldsymbol{P}\frac{\mathrm{d}\boldsymbol{Y}}{\mathrm{d}s}+\boldsymbol{Q}=\boldsymbol{0}, \tag{3}$$

where

$$\boldsymbol{P}=\mathrm{diag}(1\ \ 1\ \ 1\ \ k_x\ \ k_y\ \ k_z), \tag{4}$$

$$\boldsymbol{Y}=[F_x\ \ F_y\ \ F_z\ \ \omega_x\ \ \omega_y\ \ \omega_z]^{\mathrm{T}}, \tag{5}$$

$$\boldsymbol{Q}=\begin{bmatrix}\omega_y F_z-\omega_z F_y\\ \omega_z F_x-\omega_x F_z\\ \omega_x F_y-\omega_y F_x\\ (k_z-k_y)\omega_y\omega_z-F_y\\ (k_x-k_z)\omega_z\omega_x+F_x\\ (k_y-k_x)\omega_x\omega_y\end{bmatrix}, \tag{6}$$

where $F_{x,y,z}$—Projection of main vector of inner force,
$\omega_{x,y,z}$—Projection of curvature-twisting vector,
$k_{x,y}$—Bending rigidity of cross section along axis x, y,
k_z—Torsional rigidity of cross section along axis z.

Bring the distributed force on motional cable harness into equations. Eq. (3) can be written as

$$\boldsymbol{P}\frac{\mathrm{d}\boldsymbol{Y}}{\mathrm{d}s}+\boldsymbol{Q}+\boldsymbol{f}=\boldsymbol{0}, \tag{7}$$

where

$$\boldsymbol{f}=[f_x \quad f_y \quad f_z \quad 0 \quad 0 \quad 0]^{\mathrm{T}}, \tag{8}$$

and $f_{x,y,z}$ is the projection of distributed force on motional cable harness.

3 Numerical Solution Method

There are many ways to record the rotation of an object. The most widely used one is Euler angle. However, there might be some issues because of the singular point. Euler quaternion is another common method. It has no singular point. Therefore, it is reasonable to adopt Euler quaternion. There is no Euler quaternion in Eq. (7). To bring Euler quaternion into Eq. (7), variable substitution is necessary. According to the theory of unlimited small rotation of rigid body, curvature-twisting vector can be substituted by Euler quaternion

$$\begin{cases}\omega_x=2\left(-q_2\dfrac{\mathrm{d}q_1}{\mathrm{d}s}+q_1\dfrac{\mathrm{d}q_2}{\mathrm{d}s}+q_4\dfrac{\mathrm{d}q_3}{\mathrm{d}s}-q_3\dfrac{\mathrm{d}q_4}{\mathrm{d}s}\right),\\ \omega_y=2\left(-q_3\dfrac{\mathrm{d}q_1}{\mathrm{d}s}-q_4\dfrac{\mathrm{d}q_2}{\mathrm{d}s}+q_1\dfrac{\mathrm{d}q_3}{\mathrm{d}s}+q_2\dfrac{\mathrm{d}q_4}{\mathrm{d}s}\right),\\ \omega_z=2\left(-q_4\dfrac{\mathrm{d}q_1}{\mathrm{d}s}+q_3\dfrac{\mathrm{d}q_2}{\mathrm{d}s}-q_2\dfrac{\mathrm{d}q_3}{\mathrm{d}s}+q_1\dfrac{\mathrm{d}q_4}{\mathrm{d}s}\right).\end{cases} \tag{9}$$

Bring Eq. (9) into Eq. (7). Considering that the sum of squares of Euler quaternion is 1, a differential-algebraic equation set is obtained, including an algebraic equation and six differential equations

$$q_1^2+q_2^2+q_3^2+q_4^2=1, \tag{10}$$

$$\frac{\mathrm{d}F_x}{\mathrm{d}s}+\left(-q_3\frac{\mathrm{d}q_1}{\mathrm{d}s}-q_4\frac{\mathrm{d}q_2}{\mathrm{d}s}+q_1\frac{\mathrm{d}q_3}{\mathrm{d}s}+q_2\frac{\mathrm{d}q_4}{\mathrm{d}s}\right)F_z-\left(-q_4\frac{\mathrm{d}q_1}{\mathrm{d}s}+q_3\frac{\mathrm{d}q_2}{\mathrm{d}s}-q_2\frac{\mathrm{d}q_3}{\mathrm{d}s}+q_1\frac{\mathrm{d}q_4}{\mathrm{d}s}\right)F_y+f_x=0, \tag{11}$$

$$\frac{\mathrm{d}F_y}{\mathrm{d}s}+\left(-q_4\frac{\mathrm{d}q_1}{\mathrm{d}s}+q_3\frac{\mathrm{d}q_2}{\mathrm{d}s}-q_2\frac{\mathrm{d}q_3}{\mathrm{d}s}+q_1\frac{\mathrm{d}q_4}{\mathrm{d}s}\right)F_x-\left(-q_2\frac{\mathrm{d}q_1}{\mathrm{d}s}+q_1\frac{\mathrm{d}q_2}{\mathrm{d}s}+q_4\frac{\mathrm{d}q_3}{\mathrm{d}s}-q_3\frac{\mathrm{d}q_4}{\mathrm{d}s}\right)F_z+f_y=0, \tag{12}$$

$$\frac{\mathrm{d}F_z}{\mathrm{d}s}+\left(-q_2\frac{\mathrm{d}q_1}{\mathrm{d}s}+q_1\frac{\mathrm{d}q_2}{\mathrm{d}s}+q_4\frac{\mathrm{d}q_3}{\mathrm{d}s}-q_3\frac{\mathrm{d}q_4}{\mathrm{d}s}\right)F_y-\left(-q_3\frac{\mathrm{d}q_1}{\mathrm{d}s}-q_4\frac{\mathrm{d}q_2}{\mathrm{d}s}+q_1\frac{\mathrm{d}q_3}{\mathrm{d}s}+q_2\frac{\mathrm{d}q_4}{\mathrm{d}s}\right)F_x+f_z=0, \tag{13}$$

$$-q_2\frac{\mathrm{d}^2q_1}{\mathrm{d}s^2}+q_1\frac{\mathrm{d}^2q_2}{\mathrm{d}s^2}+q_4\frac{\mathrm{d}^2q_3}{\mathrm{d}s^2}-q_3\frac{\mathrm{d}^2q_4}{\mathrm{d}s^2}+2\frac{k_z-k_y}{k_x}\left(-q_3\frac{\mathrm{d}q_1}{\mathrm{d}s}-q_4\frac{\mathrm{d}q_2}{\mathrm{d}s}+q_1\frac{\mathrm{d}q_3}{\mathrm{d}s}+q_2\frac{\mathrm{d}q_4}{\mathrm{d}s}\right)\times\left(-q_4\frac{\mathrm{d}q_1}{\mathrm{d}s}+q_3\frac{\mathrm{d}q_2}{\mathrm{d}s}-q_2\frac{\mathrm{d}q_3}{\mathrm{d}s}+q_1\frac{\mathrm{d}q_4}{\mathrm{d}s}\right)-\frac{F_y}{2k_x}=0, \tag{14}$$

$$-q_3\frac{\mathrm{d}^2q_1}{\mathrm{d}s^2}-q_4\frac{\mathrm{d}^2q_2}{\mathrm{d}s^2}+q_1\frac{\mathrm{d}^2q_3}{\mathrm{d}s^2}+q_2\frac{\mathrm{d}^2q_4}{\mathrm{d}s^2}+2\frac{k_x-k_z}{k_y}\left(-q_2\frac{\mathrm{d}q_1}{\mathrm{d}s}+q_1\frac{\mathrm{d}q_2}{\mathrm{d}s}+q_4\frac{\mathrm{d}q_3}{\mathrm{d}s}-q_3\frac{\mathrm{d}q_4}{\mathrm{d}s}\right)\times\left(-q_4\frac{\mathrm{d}q_1}{\mathrm{d}s}+q_3\frac{\mathrm{d}q_2}{\mathrm{d}s}-q_2\frac{\mathrm{d}q_3}{\mathrm{d}s}+q_1\frac{\mathrm{d}q_4}{\mathrm{d}s}\right)+\frac{F_x}{2k_y}=0, \tag{15}$$

$$-q_4\frac{\mathrm{d}^2q_1}{\mathrm{d}s^2}+q_3\frac{\mathrm{d}^2q_2}{\mathrm{d}s^2}-q_2\frac{\mathrm{d}^2q_3}{\mathrm{d}s^2}+q_1\frac{\mathrm{d}^2q_4}{\mathrm{d}s^2}+2\frac{k_y-k_x}{k_z}\left(-q_2\frac{\mathrm{d}q_1}{\mathrm{d}s}+q_1\frac{\mathrm{d}q_2}{\mathrm{d}s}+q_4\frac{\mathrm{d}q_3}{\mathrm{d}s}-q_3\frac{\mathrm{d}q_4}{\mathrm{d}s}\right)\times\left(-q_3\frac{\mathrm{d}q_1}{\mathrm{d}s}-q_4\frac{\mathrm{d}q_2}{\mathrm{d}s}+q_1\frac{\mathrm{d}q_3}{\mathrm{d}s}+q_2\frac{\mathrm{d}q_4}{\mathrm{d}s}\right)=0, \tag{16}$$

$q_1(s)$, $q_2(s)$, $q_3(s)$, $q_4(s)$ and $F_x(s)$, $F_y(s)$, $F_z(s)$ can be obtained from the equation set. Then the coordinate of P can be obtained from the integral of Euler quaternion

$$\begin{cases}\xi(s)=2\displaystyle\int_0^s(q_2(u)q_4(u)+q_1(u)q_3(u))\mathrm{d}u+\xi(0),\\ \eta(s)=2\displaystyle\int_0^s(q_3(u)q_4(u)-q_1(u)q_2(u))\mathrm{d}u+\eta(0),\\ \zeta(s)=\displaystyle\int_0^s(q_1^2(u)-q_2^2(u)-q_3^2(u)+q_4^2(u))\mathrm{d}u+\zeta(0).\end{cases} \tag{17}$$

The profile of motional cable harness will be determined by Eq. (17).

After dimensionless processing, the equation set is discretized by differential quadrature method (DQM). DQM was first proposed by BELLMAN, et al[28–29] in 1971 and 1972. This method does not depend on variational principle and has a simple mathematical principle as well as high computational accuracy and low calculation quantity[30].

In DQM, the differential coefficient value at one point is expressed by the weighted sum of the function value of all the points

$$\left.\frac{\mathrm{d}x}{\mathrm{d}s}\right|_{s=s_i}=\sum_{k=1}^{N}A_{ik}^{(1)}x_k, \tag{18}$$

where N—Amount of the points,
A_{ik}—Coefficient,
x_k—Value of the function at point k.

Eq. (18) can be written in matrix as

$$\boldsymbol{x}^{(1)} = \boldsymbol{A}^{(1)}\boldsymbol{x}. \tag{19}$$

The 2 rank differential coefficient can be expressed by

$$\frac{\mathrm{d}^2 x}{\mathrm{d}s^2} = \frac{\mathrm{d}}{\mathrm{d}s}\left(\frac{\mathrm{d}x}{\mathrm{d}s}\right) = \sum_{k=1}^{N} A_{ik}^{(1)} \sum_{m=1}^{N} A_{km}^{(1)} x_m. \tag{20}$$

Eq. (20) can be written in matrix as

$$\boldsymbol{x}^{(2)} = \boldsymbol{A}^{(2)}\boldsymbol{x} = \boldsymbol{A}^{(1)}\boldsymbol{A}^{(1)}\boldsymbol{x}. \tag{21}$$

Use Lagrange function to be the test function. The elements of coefficient matrix can be obtained by

$$\begin{cases} A_{ij} = \dfrac{\prod\limits_{\substack{k=1 \\ k\neq i,j}}^{N} (s_i - s_k)}{\prod\limits_{\substack{k=1 \\ k\neq j}}^{N} (s_j - s_k)}, \\ A_{ii} = \sum\limits_{\substack{k=1 \\ k\neq i}}^{N} \dfrac{1}{(s_i - s_k)}. \end{cases} \tag{22}$$

There are some methods to get the points. Many studies have revealed that Chebyshev method is one of the most effective among these methods.

In Chebyshev method, the points can be obtained by

$$s_i = \frac{1-\cos[(i-1)\pi/(N-1)]}{2}a, \tag{23}$$

where a—Length of the solution region.

Then the differential equations can be discretized into algebraic equations by DQM.

There are five groups of boundary conditions, including two groups of mechanical boundary conditions, two groups of geometrical boundary conditions and one group of position boundary conditions. Three groups of the boundary conditions are required during the numerical solution method, including two groups of mechanical boundary conditions and one group of position boundary conditions or two groups of geometrical boundary conditions and one group of position boundary conditions. It is very difficult to obtain the mechanical boundary conditions because there is no effective method to measure the force at the end of the motional cable harness. The geometrical boundary conditions are easy to obtain. They can be determined by the rigid part connected with the motional cable harness. Thus the geometrical boundary conditions are preferred to be used in numerical solution method.

The boundary conditions used in numerical solution method are

$$\begin{cases} \boldsymbol{q}_o = [q_{1,0} \quad q_{2,0} \quad q_{3,0} \quad q_{4,0}], \\ \boldsymbol{q}_l = [q_{1,l} \quad q_{2,l} \quad q_{3,l} \quad q_{4,l}], \\ \boldsymbol{R}_l = [R_1 \quad R_2 \quad R_3], \end{cases} \tag{24}$$

where $\boldsymbol{q}_o$—Euler quaternion of the fixed point,
$\boldsymbol{q}_l$—Euler quaternion of the moving point,
$\boldsymbol{R}_l$—Vector from the fixed point to the moving point.

The length of the motional cable harness has to be constant during the motion simulation process. This can be ensured in the theory of the integral process described by Eq. (17). However, sometimes it is very difficult to be ensured in numerical solution process due to the limitation of the amount of points. The problem can be solved by adding this following equation into the equation set

$$L = \sum_{k=1}^{N} \sqrt{(\xi_k - \xi_{k-1})^2 + (\eta_k - \eta_{k-1})^2 + (\zeta_k - \zeta_{k-1})^2}. \tag{25}$$

Now an overdetermined equation set is obtained, including Eqs. (7) (discretized), (24) and (25). It can be solved by Levenberg-Marquardt method.

Levenberg-Marquardt method is presented by LEVENBERG[31] and reminded by MARQUARDT[32] in 1963. The algorithm of Levenberg-Marquardt method can be described as

$$\begin{cases} \mu_i = \left\| \boldsymbol{J}_i^{\mathrm{T}} \boldsymbol{F}_i \right\|, \\ \boldsymbol{d}_i = -(\boldsymbol{J}_i^{\mathrm{T}} \boldsymbol{J}_i + \mu_i \boldsymbol{D}_i^{\mathrm{T}} \boldsymbol{D}_i)^{-1} \boldsymbol{J}_i^{\mathrm{T}} \boldsymbol{F}_i, \\ \boldsymbol{x}_{i+1} = \boldsymbol{x}_i + \boldsymbol{d}_i, \end{cases} \tag{26}$$

where $\boldsymbol{J}_i$—Jacobian matrix of the equation set,
$\boldsymbol{F}_i$—Value of the equation set,
$\boldsymbol{D}_i$—Scale matrix.

The loop will not end until $\mu_i < err$.

When q_{1k}, q_{2k}, q_{3k} and q_{4k}, k=1, 2, ⋯, N, are obtained, the profile of motional cable harness can be determined by Eq. (17).

4 Motion Simulation Method

4.1 Data structure

The data structure of the motion simulation method is based on “Path” and “Profile”. “Path point” is the element of “Path”. “Node” is the element of “Profile”. “Path”, “path point”, “Profile”, and “node” are shown in Fig. 2. The “Path” in Fig. 2 is composed of 10 “path points” and the “Profile” in Fig. 2 is composed of 11 “nodes”.

The content of a “Path” is the positions and rotation matrices of all “path points” which belong to the “Path”. The structure of a “Path” is

$$\left[[\boldsymbol{r}_i^1 \quad \boldsymbol{A}_i^1] \quad [\boldsymbol{r}_i^2 \quad \boldsymbol{A}_i^2] \quad \cdots \quad [\boldsymbol{r}_i^M \quad \boldsymbol{A}_i^M]\right], \tag{27}$$

where $\boldsymbol{r}_i^k$—Position of the "path point",
$\boldsymbol{A}_i^k$—Rotation matrix of the "path point".

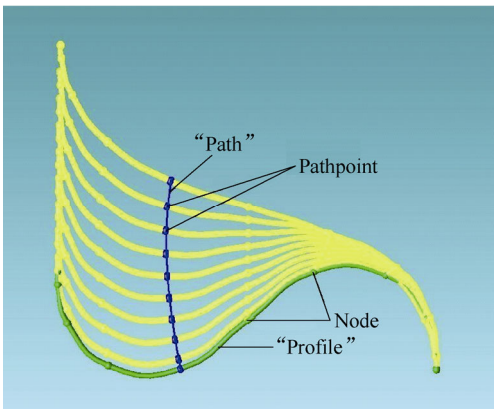

Fig. 2. "Path" and "Profile"

The content of a "Profile" is the positions and rotation matrices of all "nodes" which belong to the "Profile". The structure of a "Profile" is

$$\left[[\boldsymbol{r}_1^j \quad \boldsymbol{A}_1^j] \quad [\boldsymbol{r}_2^j \quad \boldsymbol{A}_2^j] \quad \cdots \quad [\boldsymbol{r}_N^j \quad \boldsymbol{A}_N^j]\right], \tag{28}$$

where $\boldsymbol{r}_k^j$—Position of the "node",
$\boldsymbol{A}_k^j$—Rotation matrix of the "node".

4.2 Motion simulation generation process

The motion simulation generation process contains 3 main steps: dispersion, computation and display.

The trail of the moving point is a continuous curve. A spatial step is given to disperse the trail into a series of discontinuous points. These points are called sampling points. The position and the rotation matrix of each sampling point are recorded. $\boldsymbol{q}_o$, $\boldsymbol{q}_l$ can be obtained from the rotation matrix of the fixed point and the rotation matrix of the sampling point. $\boldsymbol{R}_l$ can be obtained from the position of fixed point and the position of the sampling point. When "dispersion" is done, a list of position and rotation matrices of sampling points will be obtained. Actually, this list is the "Path" of the moving point. A "dispersion" example is shown in Fig. 3.

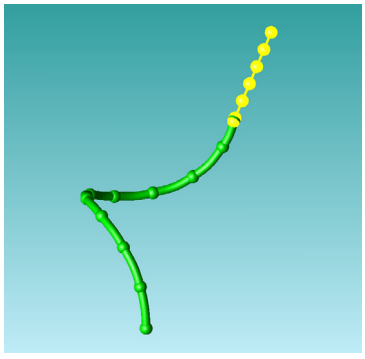

Fig. 3. Path dispersion

After the "dispersion", we need to load the position and the rotation matrix of the first sampling point for computation. Then bring the boundary conditions got from computation into the model described in section 2. Solving the equation set by the method described in section 3 is the next step. The profile of the motional cable harness is obtained. Move on to the next sampling point and repeat the operation until the last sampling point is finished. After the computation of all the sampling points, a list of "Profile" will be obtained.

"Display" is to use the "Profile" from the list one by one and display them on the screen. One problem could be caused by the discord between spatial step and temporal step. For example, suppose the spatial step is 1 mm and the temporal step is 0.02 s. The moving point moves 1 mm within 0.2 s. Thus, only the profiles at 0 s and 0.2 s will be computed. The profiles at 0.02 s, 0.04 s, $\cdots$, 0.18 s will be omitted. This will result in the display discontinuous. An interpolation method is applied to deal with this problem. The interpolated spatial step is computed by

$$\begin{cases} \Delta\xi = \dfrac{\xi_{t+\Delta t} - \xi_t}{n_{\Delta t}}, \\ \Delta\eta = \dfrac{\eta_{t+\Delta t} - \eta_t}{n_{\Delta t}}, \\ \Delta\zeta = \dfrac{\zeta_{t+\Delta t} - \zeta_t}{n_{\Delta t}}, \end{cases} \tag{29}$$

where $n_{\Delta t}$—Amount of the moments between the two sampling moments.

In this way the omitted profiles can be computed by Eq. (29).

5 Experimental Verification

A set of experimental equipments is established to verify the accuracy of the model and the effect of the simulation method presented in this paper. The measuring system of the equipments is based on binocular vision. Different components of the system are shown in Fig. 4.

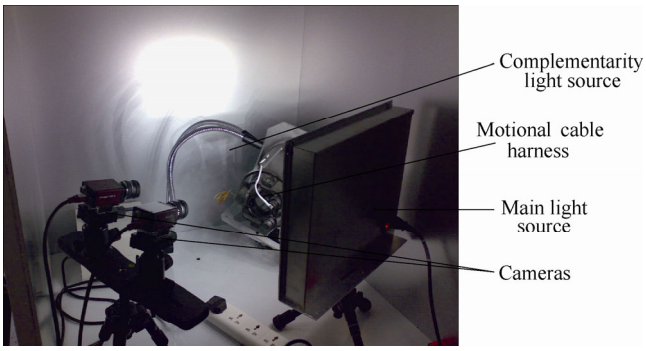

Fig. 4. Experimental equipments

The physical characteristic parameters of the motional cable harness used in the experiment are measured by

experiment and shown in Table 1. The same values were used in the simulation.

Table 1. Parameters in simulation and experiment

Parameter	Value
Bending rigidity k_x, k_y/(mN • m^2)	0.134 5
Torsional rigidity k_z/(mN • m^2)	2.448
Diameter d/mm	4
Length l/m	0.18
Density ρ/(kg • m^{-3})	557.1

The motional cable harness is a beeline and turns 180° widdershins at one end from origin. The mechanical boundary conditions described in $O\xi\eta\zeta$ coordinate system are shown as follows, $P_0(0, 0, 0)$, $\boldsymbol{i}_0=(0, 0, 1)$, $\boldsymbol{j}_0=(1, 0, 0)$, $\boldsymbol{k}_0=(0, 1, 0)$, $P_1(0, 1, 0)$, $\boldsymbol{i}_1=(0, 0, -1)$, $\boldsymbol{j}_1=(-1, 0, 0)$, $\boldsymbol{k}_1=(0, 1, 0)$. Then one end moves toward the other. The comparison pictures between simulation and experiment are shown in Fig. 5. It can be seen that the cable harness deformation of wrapping from twist in both virtual and real environments. And the deformation occurred at the same position of the cable with the same extent.

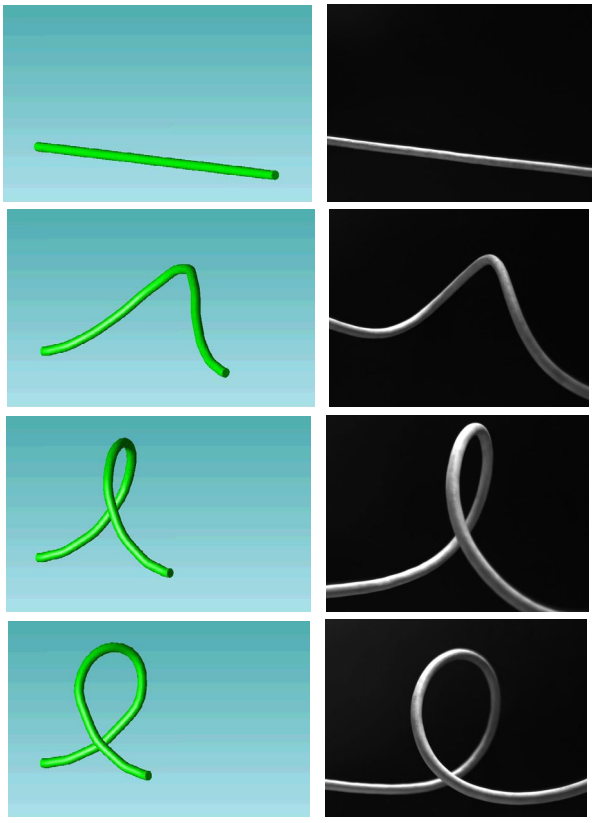

Fig. 5. Comparisons between simulation and experiment

The experiments in different degrees are also implemented. The trend of the motion is almost the same as the one at 180°. Only the extent is a little different. One thing should note that the model proposed in this paper can be used only within 360°.

The motional cable harness is quite different from the object focused on in the previous mechanical study because of its strong flexibility. It is validated by the experiment that the model presented in this paper can describe the complex profile of motional cable harness accurately and the simulation method is effective.

6 Prototype System for Motional Cable Harness Design

A prototype system named "Motional Cable Harness Design and Simulation System (MCHDS)" is developed based on the physics-based model and simulation method presented in this paper. This system is a part of "Virtual Assembly Process Planning (VAPP)" system. Engineers can design as well as simulate the motion process of motional cable harness to predict any problems there might be. The flow chart of design and motion simulation is shown in Fig. 6.

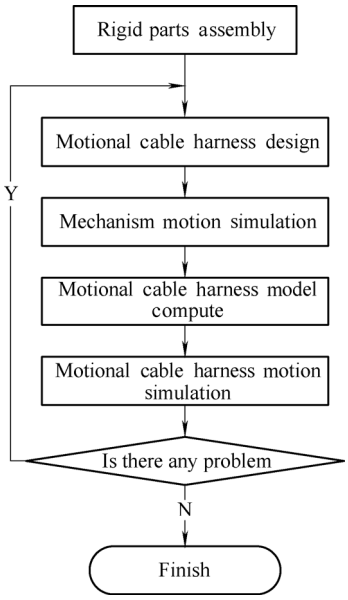

Fig. 6. Flow chart of design and motion simulation

With the developed prototype system, a comparison between the original design and modified design is shown in Fig. 7. The original design with an apparent collision (left in Fig. 7) was redesigned by lengthening the motional cable harness. Then the new collision-free design is shown in the right picture.

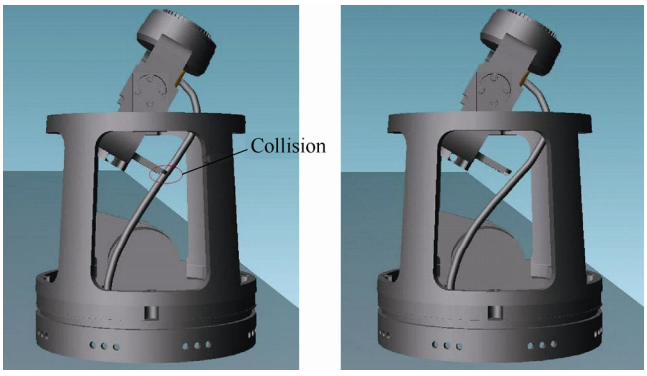

Fig. 7. Comparison between the original design and modified design

7 Conclusions

(1) In this paper, a physics-based model of motional cable harness based on elastic rod theory is presented. The model was verified more accurate and effective than geometric model and spring-mass model when simulating the deformation of this special kind cable harness.

(2) A set of experimental equipments was established along with the motion simulation method. According to the comparison between the simulation result and experimental result, the experimental verification system and the simulation system are reliable.

(3) The developed system is a new efficient motional cable harness design tool in avoiding many potential issues, which is of crucial importance in more and more complex products.

References

[1] RABAETJE R. Real-time simulation of deformable objects for assembly simulations[C]//*Proceedings of the Fourth Australasian User Interface Conference on User Interfaces*, Adelaide, Australian, 2003, 18: 57–64.

[2] LEON J C, GANDIAGA U, DUPONT D. Modeling flexible parts for virtual reality assembly simulations which interact with their environment[C]//*Proceedings International Conference on Shape Modeling and Applications*, Genova, Italy, 2001: 335–344.

[3] LOOCK A, SCHOMER E. A virtual environment for interactive assembly simulation: from rigid bodies to deformable cables[C]//*5th World Multiconference on Systemics, Cybernetics and Informatics (SCI 2001)*, Orlando, USA, 2001(3): 325–332.

[4] HERGENROTHER E, DAHNE P. Real-time virtual cables based on kinematic simulation[C]//*Conference Proceedings of the WSCG*, Plzen, Czech Republic. Univ. West Bohemia, 2000, 2: 402–409.

[5] QI Luo, JING Xiao. Haptic rendering involving an elastic tube for assembly simulations[C]//*Proceedings of the IEEE International Symposium on Assembly and Task Planning*, Montreal, QC, Canada, 2005: 53–59.

[6] SANG Y K, JINAH P, DONG S K. Multiple-contact representation for the real-time volume haptic rendering of a non-rigid object[C]//*Proceedings of 12th International Symposium on Haptic Interfaces for Virtual Environment and Teleoperator Systems*, Chicago, Illinois, USA, 2004: 242–249.

[7] SEONGKI J, JINBOK C, MAENGHYO C. Physics-based s-adaptive haptic simulation for deformable object[C]//*Symposiun on Haptic Interfaces for Virtual Environment and Teleoperater Systems*, Alexandria, Virginia, USA, 2006: 477–483.

[8] ZAJAC E E. Stability of two planar loop elasticas[J]. *Journal of Applied Mechanics*, 1962, 29(1): 136–142.

[9] COHEN H. A nonlinear theory of elastic directed curves[J]. *International Journal of Engineering Science*, 1966, 4(5): 511–524.

[10] JAMES R D. The equilibrium and post-buckling behavior of an elastic curve governed by a non-convex energy[J]. *Journal of Elasticity*, 1981, 11(3): 239–269.

[11] KNAP R H. Derivation of a new stiffness matrix for helically armoured cables considering tension and torsion[J]. *International Journal for Numerical Methods in Engineering*, 1979, 14(4): 515–529.

[12] KNAPP R H. Helical wire stresses in bent cables[J]. *Journal of Offshore Mechanics and Arctic Engineering*, 1988, 110(1): 55–61.

[13] COYNE J. Analysis of the formation and elimination of loops in twisted cable[J]. *Journal of Oceanic Engineering*, 1990, 15(2): 72–83.

[14] LE T T, KNAPP R H. A finite element model for cables with nonsymmetrical geometry and loads[J]. *Journal of Offshore Mechanics and Arctic Engineering*, 1994, 116(1): 14–20.

[15] MIYAZAKI Y, KONDO K. Analytical solution of spatial elastica and its application to kinking problem[J]. *International Journal of Solids and Structures*, 1997, 34(27): 3619–3636.

[16] VAN DER HEIJDEN G H M, CHAMPNEYS A R, THOMPSON J M T. The spatial complexity of localized buckling in rods with noncircular cross section[J]. *SIAM Journal on Applied Mathematics*, 1998, 59(1): 198–221.

[17] VAN DER HEIJDEN G H M, THOMPSON J M T. Lock-on to tape-like behavior in the torsional buckling of anisotropic rods[J]. *Physica D: Nonlinear Phenomena*, 1998, 112(1–2): 201–224.

[18] VAN DER HEIJDEN G H M, THOMPSON J M T. Helical and localized buckling in twisted rods: A unified analysis of the symmetric case[J]. *Nonlinear Dynamics*, 2000, 21(1): 71–99.

[19] SEEMANN W. Deformation of an elastic helix in contact with a rigid cylinder[J]. *Archive of Applied Mechanics*, 1996, 67(1–2): 117–139.

[20] VAN DER HEIJDEN G H M, CHAMPNEYS A R, THOMPSON J M T. Spatially complex localization in twisted elastic rods constrained to lie in the plane[J]. *Journal of the Mechanics and Physics of Solids*, 1999, 47(1): 59–79.

[21] VAN DER HEIJDEN G H M. The static deformation of a twisted elastic rod constrained to lie on a cylinder[J]. *Proceedings of the Royal Society of London*, 2001, 457(2007): 695–715.

[22] VAN DER HEIJDEN G H M, CHAMPNEYS A R, THOMPSON J M T. Spatially complex localisation in twisted elastic rods constrained to a cylinder[J]. *International Journal of Solids and Structures*, 2002, 39(7): 1863–1883.

[23] BENHAM C J. Elastic model of supercoiling[J]. *Proceeding of the National Academy of Sciences of the USA*, 1977, 74(6): 2397–2401.

[24] BENHAM C J. An elastic model of the large-scale structure of duplex DNA[J]. *Biopolymers*, 1979, 18(3): 609–623.

[25] LE BRET M. Relationship between the energy of superhelix formation, the shear modulus, and the torsional brownian motion of DNA[J]. *Biopolymers*, 1978, 17(8): 1939–1955.

[26] LE BRET M. Catastophic variation of twist and writhing of circular DNAs with constraint[J]. *Biopolymers*, 1979, 18(7): 1709–1725.

[27] LIU Yanzhu. *Nonlinear mechanics of thin elastic rod*[M]. Beijing: Tsinghua University Press, 2006.

[28] BELLMAN R, CASTI J. Differential quadrature and long term integration[J]. *Journal Mathematical Analysis and Application*, 1971, 34(2): 235–238.

[29] BELLMAN R, KASHEF B G, CASTI J. Differential quadrature: a technique for the rapid solution of nonlinear partial differential equations[J]. *Journal of Computation Physics*, 1972, 10(1): 40–52.

[30] CHENG Changjun, ZHU Zhengyou. Recent advances in differential quadrature method with applications to mechanics[J]. *Journal of Shanghai University*, 2009, 15(6): 551–559.

[31] PUJOL J. The solution of nonlinear inverse problems and the Levenberg-Marquardt method[J]. *Geophysics*, 2007, 72(4): W1–W16.

[32] MARQUARDT D W. An algorithm for least-squares estimation of nonlinear parameters[J]. *Journal of the Society for Industrial and Applied Mathematics*, 1963, 11(2): 431–441.

Biographical notes

LIU Jianhua, is a professor, PhD advisor, and he received his PhD degree in Mechanical Engineering from *Beijing Institute of Technology, China*. His scholastic interests include virtual assembly and virtual reality. Now he has published over 60 research papers in virtual assembly.

ZHAO Tao, born in 1985, is currently a master candidate. His research interests include cable harness modeling based on

physical characteristic.

NING Ruxin is a professor, PhD advisor, and she received her PhD degree in Mechanical Engineering from *Technical University of Berlin, Germany*. Her research field is digital design and manufacture. Now she is the Academically-Chairman of Mechanical Engineering of Beijing Institute of Technology, President of Production Engineering Society of the Chinese Mechanical Engineering Society.

LIU Jiashun is currently a PhD candidate at *Beijing Institute of Technology, China*. His research interests include cable harness modeling and assembly simulation.